EUROPEAN ORGANIZATION FOR NUCLEAR RESEARCH

NP Internal Report 61 - 11
Internal circulation only.
Not for publication.

RESULTS OF THE FIRST NEUTRINO COUNTER BACKGROUND RUNS

by

H. Faissner, F. Ferrero and M. Reinharz.

***

SUMMARY

The charged particle background present in the "neutrino blockhouse" has been studied with several large-area scintillation and Čerenkov counter set-ups, and under various shielding and PS conditions. Most of the background seems to be due to muons which do not come along the line of sight from target 5, but rather penetrate through weak parts of the neutrino shielding on the side of this line. The background increases strongly with PS energy. Approximately the same energy dependence has been found, in a separate experiment, for the flux of muons capable of penetrating 23.5 m of heavy concrete.

Geneva - July, 1961.

1896/NP/kw

RESULTS OF THE FIRST NEUTRINO COUNTER BACKGROUND RUNS

I. INTRODUCTION

The neutrino counter background runs took place on the following dates:

Run 1	:	6 -13 February 1961	(12 shifts)
Run 2*)	:	14-16 April 1961	(8 shifts)
Run 3	:	20-21 May 1961	(2 shifts)
Run 4	:	2 -5 June 1961	(11 shifts).

The measurements were done in the north-west corner of the PS South Hall under various shielding conditions (see Section II). Using a relatively small counter arrangement (see Section III), it was checked in Run 1 that the counters work satisfactorily, and that the method of measurement foreseen for the neutrino counter experiment[1] is practicable. Muon fluxes were measured at various PS energies and behind different shielding thicknesses (see Figs. 7 and 8). A systematic study of the charged particle background was started. It was continued with basically the same set-up, but better shielding conditions, during Run 2. The counter arrangement was considerably enlarged for Runs 3 and 4, in order to incorporate the multiplate cloud chamber. We include some of the counter data in the present report. The final report on Run 4 will be issued as soon as the scanning of cloud chamber pictures is finished[2]. The main results on the background as seen by the counters are summarized in Figs. 9 and 10 and in Tables I - V.

II. SHIELDING CONDITIONS

Run 1 took place underneath the overhanging roof, in the position which at present is occupied by the Ecole Polytechnique bubble chamber (Fig. 1). The main shielding wall between the PS

*) Run 2 was done by parasiting on the background run of the Ecole Polytechnique bubble chamber.

ring and South Hall was still intact. A wall of heavy concrete was put in front of the counters. Its thickness was increased during the run from initially 4.80 m to 11.2 m (up to a height of 80 cm the full thickness was in place all the time). The side shielding was only provisional. It was 4 m high, but did not join to the overhanging roof, thereby leaving a gap open which was $\approx$ 1 m at the front and several metres at the rear part of the overhanging roof, where it joined the "Chinese wall".

During Run 2, major parts of the final shielding were already in place (Fig. 2). The recess in the main shielding wall was made and closed with the 4.32 m thick iron plug (except for the 112 cm^2 muon channel, which could be closed by three times 1 m of Pb mounted on moveable chariots). The counters were in their final position, and the surrounding blockhouse was practically finished.

For Run 3 additional shielding was added (indicated in black in Fig. 3). Most of it was placed inside the ring, in particular around magnet No. 10 from where neutron background was found to emerge by the Ecole Polytechnique bubble chamber group[3].

For Run 4 a few more concrete blocks were added near the "weak corner" of the shielding wall between the PS ring and South Hall (marked A in Fig. 3).

III. COUNTER ARRANGEMENTS

The set-up used in Run 1 was the so-called "short sandwich" (Fig. 4), consisting of two liquid scintillation YES-counters, Y_1 and Y_2, behind 30 and 35 cm Pb, respectively, followed by another 5 cm Pb and a directional water Čerenkov counter C. The area of the YES-counters was 1.6 × 0.8 m^2, the area of the Cerenkov counter 1.8 × 1.2 m^2 *). These counters were protected by a 1.6 × 2.4 m^2

*) Accidentally only the upper half of this counter was connected to the coincidence circuit.

FRONT-counter F and a TOP-counter T, which was 1.6 × 1.6 m² in the horizontal and 1.1 × 1.0 m² in the inclined part. There was a 20 cm Fe roof between YES-sandwich and TOP-counter. Some information about charged particles coming from the sides was provided by two plastic counters (1.0 × 0.5 m² and 0.7 × 0.7 m²) on the left-hand side, and one scintillation tank 1.6 × 0.8 m² on the right-hand side*).

In Run 2 the arrangement was basically the same, except that the final side anticoincidence counters of 1.6 × 2.4 m² area were now in place, and that some of the counters started to leak. Therefore, only one YES-counter was used behind 40 cm Pb (Fig. 5), and on the average only two-thirds of the counter units composing the FRONT, LEFT- and RIGHT-counters were working. The Čerenkov counter instead was now 100% effective. The TOP-counter of now 1.6 × 2.4 m² was working all the time.

For Run 3 a new arrangement was set up which could trigger the cloud chamber (Fig. 6). The FRONT-counter is now 2.4 × 4.0 m², the side counters have the same size as in Run 2. Systematic measurements were only made with the Čerenkov counter C_B (2.4 × 1.6 m²) and the scintillation counters Y_B (3.0 × 1.8 m²) as YES-counters. The TOP-counter of 4.0 × 4.0 m² was not yet in place.

The geometry in Run 4 was practically the same as in Run 3. The TOP-counter was in operation, and also the additional YES-counters C_L,Y_L and C_R,Y_R were used (sensitive areas of $C_{L,R}$ = 1.6 × 2.4 m²; of $Y_{L,R}$ = 1.0 × 1.8 m²). Due to the better mechanical construction of the new counters no breakdown has occurred up to now. Also, the transistorized electronics used with the new set-up proved very reliable and stable.

IV. RESULTS OF RUN 1

1. Muon fluxes from target 5

A muon above ≈ 1 GeV, when transversing the short sandwich, would cause a triple coincidence $(Y_1\ Y_2\ C)^3$. This coincidence rate

*) "Right" and "left" as seen when facing target No. 5.

was measured as a function of PS energy at a fixed total shielding thickness of 23.5 m heavy concrete (which, together with the detector threshold, gives a momentum cut-off at 17.7 GeV/c). 50 μm Be and 25 μm Al were used as targets. The result is given in Fig. 7: between 18 and 23 GeV the muon fluxes rise by a factor of ≈ 3 per GeV energy increase, and somewhat less fast for the higher energies. The Be to Al ratio is consistent with 2.0 at all energies where measurements were done, except the highest one (27.8 GeV) where it is only 1.5. The point marked KSS in Fig. 7 refers to a calculation by Krienen, Salmeron and Steinberger[4] done on the basis of a statistical pion spectrum as given by von Behr and Hagedorn[5]. Magnetic effects and multiple scattering were not considered in the calculation.

Another measurement was made with Be at a fixed PS energy of 24.3 GeV during the time when more shielding was piled up in front of the counters. Up to a cut-off momentum of $\approx$ 20.5 GeV the muon flux follows quite closely to what is expected from the statistical spectrum (Fig. 8). Yet the good agreement with the calculation of Krienen et al.[4] must be considered as accidental: in fact, one does not get muons from pions originally emitted under $\sim 6°$ from the target but rather mostly negative muons from negative pions emitted under small angles which are bent outward by the PS fringing field[6].

The measured curve does not show the expected sharp cut-off at $\approx$ 21 GeV/c. This is a strong indication that, at these big shielding thicknesses, one measures charged particles which do not come straight from target 5.

2. "Neutrino"-triggers as a function of shielding thickness

Simultaneously with the muon fluxes, the rates of "neutrino-like" anticoincidences, $\bar{F}(Y_1\ Y_2\ C)^3$, were measured. They follow the measured charged particle fluxes quite closely (Fig. 9), indicating nothing but the inefficiency of the anticoincidence system. This

inefficiency is only in part due to the electronics; the main contribution comes from particles which missed the sensitive parts of the FRONT-counter F. The levelling-off of the observed rates at high shielding thicknesses shows again that one measures particles which do not come directly from target 5.

3. Analysis of background by display of counter pulses

As soon as the anticoincidence rate was lower than 1 per burst, the pulses from all the counters with suitable delays between them were displayed on an oscilloscope and photographed, using the "neutrino-like" anticoincidence as a trigger. In this way the electronical inefficiency can be determined directly by comparing the number of oscilloscope traces showing NO-counter pulses on them with the number of coincidences registered during the same time*). By observing which ones of the NO- and YES-counters have responded to a particular event, a rough hodoscope is realized. Finally, the pulse heights can be used for further discrimination, for instance between penetrating particles and showers.

The hodoscopic information obtainable from the display depends on the trigger signature chosen. If one triggers with an anticoincidence $\overline{A_1}\ \overline{A_2}\ldots\overline{A_n}(YC)^2$ the fraction of traces showing a particular NO-counter A_K on them is proportional to the flux of particles through this counter [and causing a double coincidence $(YC)^2$] times the inefficiency of this counter to close the anticoincidence circuit. Although care was taken to ensure equal overall gain for all the NO-counters, occasionally slight differences of the anticoincidence efficiencies were observed for different counters. Unbiased data on the distribution of charged background particles can be obtained by choosing only combinations of YES-counter pulses as a trigger.

---

*) It was found to be $(3 \pm 0.5) \times 10^{-3}$ for both, triples $\bar{F}(Y_1\ Y_2\ C)^3$ and doubles $\bar{F}(Y_1\ Y_2\ C)^2$, when the muon flux was of the order of 10 per m^2 and burst. It was worse during the later stages of Run 1 and in Run 2, mainly because of changes in the biases, etc.

4. Depression of cosmic-ray background

The first systematic background study, using the display, was made with the completed shielding (muon cut-off momentum 21.3 GeV/c) and a long radiation burst (gate length 50 msec). The trigger was $\bar{F}(Y_1\ Y_2\ C)^2$, i.e., a double coincidence between any of the three YES-counters in anticoincidence with the FRONT-counter F.

There was a pronounced difference between cosmic-ray background and background from the PS: cosmic rays produced mainly coincidences between the two scintillators $(Y_1\ Y_2)^2$, whereas with the PS operating at 24 GeV a high fraction of coincidences $(Y_2\ C)^2$ was found, too. In order to depress the cosmic-ray background, the radiation burst length was shortened to some msec by exchanging the thin targets against ones of ≈ 1 mm thickness. It was checked that counters and electronics worked well with the short burst, and that the rate of accidental coincidences was still negligible*).

The results with the short burst are given in Table I. The difference between the PS background and cosmic rays is striking. The PS background particles come from the forward direction*) (in the loose sense that angles up to $\approx 30°$ with respect to the ν-direction are still accepted). Most of them are presumably muons which missed the FRONT-counter (and therefore Y_1), but still hit Y_2 and C.

5. Background under different PS conditions

In order to get more information about the machine background, the PS energy and the target material were varied. The results, as given in Table I, reveal the following properties of background:

a) The already-mentioned directionality of the PS background at 24 GeV. This is demonstrated by the high fraction of $(Y_2\ C)^2$ coincidences amongst the "good triggers", as well as by the high efficiency of the FRONT-counter as compared to all the other NO-counters.

---

*) The contrary was erroneously stated by one of us (H.F.) in a preliminary discussion of the results on 23 February, 1961 (see document NP/765/EB).

b) The comparison between Be and Al at 24 GeV gives the same factor of 2 already found in the high-energy tail of the muon spectrum (Fig. 7).

c) The background depends strongly on the PS energy: between 24 and 19 GeV the coincidence rate goes down by a factor of 22 for Be. At the same time, the directionality is lost and the Be-Al difference vanishes. In fact, the coincidence rate at 19 GeV is not significantly different from cosmic-ray level. Surprisingly enough, there seems to be a definite PS effect in the anticoincidence rate.

d) The single counting rates per burst are given in Table II. Also they show a pronounced energy dependence. (Care must be taken in the comparison, as fluctuations in PS intensity could not be corrected for because of lack of a convenient monitor.) When the PS is on, the counting rate in the practically unshielded scintillation counter Y_2 is significantly higher than the one in the well-protected counter Y_1. This indicates the presence of a non-directional, soft radiation, as it was already found in a preliminary radiation survey in the South Hall[7]. The low counting rate in the Čerenkov counter would be consistent with the assumption that most of these background particles are neutrons.

V. RESULTS OF RUN 2

Because of the changes in geometry and electronics, the data of this run are not directly comparable to the ones of Run 1. However, for the $(Y\ C)^2$ rates, the conditions were not too different and a comparison of these would indicate a depression of background by approximately an order of magnitude.

The main emphasis during this run was on triggering the display by a very loose trigger, namely, singles from either Y or C (or both), or antisingles (i.e., singles in anticoincidence with the NO-counters). The intention was to get an unbiased distribution of the particle directions. Actually, the singles rates given in

Table III still contain a bias: the discrimination level was set as high as to exclude practically particles under normal incidence, admitting only inclined ones. As a result, the absolute counting rates are too low, and the fraction of particles coming from the sides is again an upper limit rather than the true value.

VI. RESULTS OF RUNS 3 AND 4

Run 3 was a short pre-run in order to check if one can trigger the cloud chamber at reasonable rates. The chamber was not yet working. The counting rates obtained with the TOP-counter missing and using only the YES-counters C_B and Y_B in the back of the cloud chamber are given in Table IV. No oscilloscope traces were photographed. The trigger rate is still approximately a factor of 5 too high for the chamber.

In order to depress the trigger rate further, the following changes were made between Runs 3 and 4:

a) the gaps in the FRONT-counter were closed to a large extent by placing a rectangular scintillation counter 2.4 × 0.8 m^2 in front of the vertical gap in the counter, and four tubes 30 cm Ø and 90 cm long across the horizontal gaps;

b) some more concrete blocks were added in the South Hall near the corner marked (A) (Fig. 3).

The third change was that due to a breakdown of the excitation of the PS magnets. As a consequence

c) the PS ran at 22.2 GeV maximum.

All three changes together brought the trigger rate down by a factor of ≈ 10. There is little doubt that the main effect came from the reduced PS energy.

With the improved FRONT-counter the anticoincidence efficiency against machine background is around 98%. Against cosmic rays it is less because part of the counters are standing outside the

anticoincidence house. In fact, cosmic rays constituted the main background during this run (see Table V). This was due in part to the loose logics employed: in order to ensure maximum detection efficiency for neutrino events, the out-puts of all Čerenkov counters and of all scintillation YES-counters were respectively added together and then mixed into a $(Y\ C)^2$ coincidence. This gives a factor of 10 more than $(Y_B\ C_B)^2$ alone, because one also counts now cosmic-ray particles travelling $\approx$ normal to the 6° line, and avoiding the NO-counters. By demanding separate coincidences $(C_B\ Y_B)^2$, $(C_L\ Y_3)^2$, and $(C_R\ Y_4)^2$ this effect can easily be avoided.

The relevant counting rate, therefore, is $\bar{A}(C_B\ Y_B)^2$. The result is quite promising, in particular at 20 GeV where the machine effect, which incidentally only shows up in the back counters, has virtually disappeared. Because the cosmic-ray background was so important this time also a pulse height criterion was imposed for an event to be "neutrino-like": the pulse height in C_B (Y_B) must not exceed two (three) times the most probable value for a transversing single particle.

VII. CONCLUSIONS

The measurements have revealed a fairly strong charged particle background even after the shielding foreseen for the neutrino experiment had been completed. It seems that most of these particles are muons. Most of the so-called "neutrino-like" triggers registered by the counters (if not all of them) are actually due to charged particles which have missed the anticoincidence counters. Only at 19 GeV PS energy there seems to be an indication of a less trivial sort of background (see Table I).

Most of the background particles come within $\pm \approx 30°$ from the 6° line to target 5. Yet they do not come directly along this line. This is clear from the amount of shielding placed on this line: it corresponds to a muon momentum cut-off $\approx$ 21.5 GeV/c. Experimentally, it has been found that above a cut-off of $\approx$ 20 GeV/c

the background rate becomes independent of the amount of shielding in the line of sight to target 5. The conclusion is then that the background particles go around the main part of the neutrino shielding, rather than through it*).

The background shows a pronounced increase with the PS energy. The data are summarized in Fig. 10. Only the counting rates from the same run are strictly comparable, because geometry and electronics changed from run to run. One finds the same trend in all runs and for all trigger signatures. It coincides with the PS energy dependence of the muon flux which was given in more detail in Fig. 6.

The present background study is only the very first step in the neutrino counter experiment. The muon background was so high that at 24 GeV it overshadowed all other background effects completely. The only definite indication of another type of PS background was found at 19 GeV**). It remains to be seen what sorts of background will show up, as soon as the weak spot (X) in the present shielding has been closed.

Some practical conclusions can already be drawn from the present measurements:

A neutrino experiment with counters alone would be extremely hard. One has to combine them with a track-showing device. A fast one, like a spark chamber, can presumably be triggered by single counters, thereby achieving high detection efficiency. A slow device, like the cloud chamber, instead requires quite restrictive signatures. A good anticoincidence efficiency is essential in both cases. It is felt that the 98% achieved for scintillator-Čerenkov coincidences are close to the practical limit obtainable with the present method of constructing the large NO-counters from smaller standard units.

---

*) Since this report was written, strong evidence has been accumulated during Run 5 (14 - 17.7.61) that the muons penetrate through the point marked X in Fig. 3. They reach the counters after deflection by multiple scattering but miss Lagarrigue's bubble chamber!

**) More systematic measurements at this energy would have been desirable, but they were not permitted by the bubble chamber groups which ran in parallel.

Another conclusion may be drawn about the PS energy to be chosen for the neutrino experiments. It has been realized already that the neutrino flux per sec has a maximum at 21 GeV: one loses a factor of 1.3 in going from 24 to 21 GeV[8,9], but gains a factor of 1.5 from the enhanced repetition rate. The present measurements seem to indicate that, as far as the signal-to-noise ratio is concerned, an even lower PS energy might be still more advantageous.

*

ACKNOWLEDGEMENTS

The authors are indebted to the PS machine group under the direction of P. Germain for their outstanding collaboration during the runs. They acknowledge in particular the excellent job done by Dr. Bonaudi and his staff with installation and shielding, by Mr. Krőwerath and his crew with the transport, and by Dr. Sluyters with the targets. Much help and guidance was provided by the "Neutrino Committee", with Professor Bernardini and Dr. Hine as chairmen, and Drs. Krienen and Salmeron as co-ordinators. The support from Professor Preiswerk and the co-operation of Dr. Astbury and the cloud chamber group is gratefully acknowledged. We wish to thank our technicians Mr. Doughty and Mr. Jørgensen, and their helpers, who worked extremely efficiently and very often up to the limits of their powers, Mr. Cucančič who contributed essential parts of the electronics, and Dr. A. Ghani who assisted during the last two runs.

* * *

REFERENCES

1) H. Faissner, NP Internal Report 61-6 (1961).

2) Counter Cloud Chamber Collaboration, NP Internal Report (in preparation).

3) Results of the background pre-runs of the Ecole Polytechnique Freon Bubble Chamber (several Internal Reports).

4) F. Krienen, R.A. Salmeron and J. Steinberger, PS/Int. EA 60-10 (1960).

5) J. von Behr and R. Hagedorn, CERN Report 60-20 (1960).

6) This was first pointed out by J. Geibel (private communication) and later checked by Lagarrigue's bubble chamber group [see Ref. 3)].

7) H. Faissner, B.D. Hyams and W.A. Love, Preliminary Radiation Survey for the Neutrino Experiment, May-June 1960 (unpublished).

8) G. von Dardel, R. Mermod, K. Winter, G. Weber and M. Vivargent, Measurements of the charged pion spectrum (private communication).

9) M. Fidecaro, G. Finocchiaro, G. Gatti, G. Giacomelli, W.C. Middelkoop and T. Yamagata, Measurements of the γ-spectra from the decay of π^0's (private communication).

* * *

Table Ia

Coincidence rates in Run 1.

(All rates per 1000 bursts; 1 burst = 2×10^{11} circulating protons in all the tables.) The rates given in the first four columns were read directly from the scalers. The relevant anticoincidence rate, given in the last column, was determined from the oscilloscope traces.

PS energy (GeV)	Target	Gate	$(Y_1Y_2\check{C})^2$	$\bar{F}\bar{T}\bar{R}(Y_1Y_2\check{C})^2$	$(Y_1Y_2\check{C})^3$	$\bar{F}\bar{T}\bar{R}(Y_1Y_2\check{C})^3$	$\overline{FTLR\ C_b}^{*)}(Y_1Y_2C)^2$
24.3	Al	3 ms	760 ± 20	148 ± 10	-	-	43 ± 5
24.3	Be	10 ms	1560 ± 50	304 ± 20	-	-	100 ± 13
24.3	Be	50 ms	-	-	420 ± 30	6 ± 3	-
19.0	Al	5 ms	81 ± 10	33 ± 4	-	-	16 ± 4
19.0	Be	5 ms	68 ± 7	30 ± 4	-	-	27 ± 5
Cosmics		5 ms	67 ± 2	18 ± 1	1.9 ± 0.04	0.23 ± 0.01	13 ± 1

Table Ib

Analysis of oscilloscope traces.
(Gate length 3 msec, target aluminium**)

PS energy (GeV)	Trigger signature	Anticounter percentage of total number of triggers					% of ν-like events	Counter combinations for ν-like events (%)	
		F	T	L	R	C_b*)		$(Y_1Y_2)^2$	$(Y_2\check{C})^2$
24.3	$\bar{F}\bar{T}\bar{R}(Y_1Y_2\check{C})^2$	53	2	4	4.5	5.5	31	8	86
19.0	$\bar{F}\bar{T}\bar{R}(Y_1Y_2\check{C})^2$	17	3	3	9	27	41	73	27
Cosmics	$\bar{F}\bar{T}\bar{R}(Y_1Y_2\check{C})^2$	11	2	2	2.5	34	48.5	84	12
Cosmics	$\bar{F}\bar{T}\bar{R}(Y_1Y_2\check{C})^3$	23	0.5	0.5	2	63	11	-	-

*) C_b is a signal from the "bad" side of the Čerenkov counter, i.e., from the phototubes looking at particles entering the set-up from behind.

**) There is no significant difference when beryllium is used.

Table II

Single counting rates in Run 1
(per 1000 bursts)

PS energy (GeV)	Target *)	Gate	č	Y_1	Y_2	Y_2/Y_1	Remarks
24	Al 5	3 ms	2750 ± 400	9800 ± 700	25300 ± 1100	2.58	-
24	Al 5	3 ms	4150 ± 450	12200 ± 800	41050 ± 1430	3.35	-
24	Be 5	10 ms	5100 ± 500	18750 ± 970	48750 ± 1560	2.60	-
19	Be 5	5 ms	3970 ± 360	2530 ± 290	4400 ± 390	1.75	low intensity
19	Al 5	5 ms	2900 ± 310	6730 ± 470	29000 ± 1000	4.30	-
Cosmics		3 ms	2040 ± 7	256 ± 3	318 ± 3	1.14	-

*) The number behind the target material refers to the straight section in which the target was placed.

Table III a

Counting rates in Run 2 (per 1000 bursts).
$\bar{A}$ means anticoincidence with F,T,L, and R.

PS energy (GeV)	Target	Gate	Scaler Y	Scaler C	Scaler $(YC)^1$	Scaler $\bar{A}(Y)^1$	Scaler $\bar{A}(C)^1$	Scaler $\bar{A}(Y,C)^1$	Scaler $(YC)^2$	Scaler $\bar{A}(YC)^2$ *)	Traces $\overline{FTLR\ C_b}\ (YC)^2$	Traces $\overline{FTLR\ C_b}\ (YC)^1$
27	Be 5	1 ms	-	-	4900 ± 300	-	-	-	2650 ± 220	1320 ± 105	66 ± 47	-
24	Be 5	1 ms	212 ± 18	880 ± 40	1050 ± 20	205 ± 70	670 ± 37	960 ± 15	146 ± 20	43 ± 2	37 ± 2	660 ± 36
24	Al 2	5 ms	-	-	2020 ± 50	-	-	1650 ± 80	14.3 ± 4	4.7 ± 2.5	6.5 ± 3	-
24	Al 10	1 ms	366 ± 20	-	-	325 ± 19	-	-	4.5 ± 2	0.7 ± 1	1 ± 1	-
21	Be 5	1 ms	128 ± 7	-	320 ± 10	102 ± 10	-	280 ± 10	7 ± 1	5.7 ± 3	6.5 ± 3	-
cosmics		1 ms	41 ± 0.6	220 ± 3	250 ± 3	16 ± 5	170 ± 20	180 ± 16	2.8 ± 0.07	0.8 ± 0.04	-	-

Table III b

Analysis of oscilloscope traces for Run 2

PS energy (GeV)	Target	Trigger signature	Anticounter percentage of total number of triggers					% of ν-like events
			F	T	L	R	C_b	
24	Be 5	$(YC)^2$	78	2	2	1	2	15
24	Be 5	$(Y)^1$	32	9	4	4	1	50
24	Be 5	$(YC)^1$	23	4	8	1	2	62
24	Be 5	$\bar{A}(YC)^1$	0.5	0.3	0.5	0.8	0.8	97
24	Be 5	$\bar{A}(Y)^1$	3	1	1	1	1	91

*) Corrected for missing parts of the front counter F.

Table IV

Counting rates in Run 3 (per 1000 bursts). The target was Be. $\bar{A}$ stands for anticoincidence with F,L, and R.

PS energy (GeV)	Target	Gate	$(C_B Y_B)^1$	$(Y_B C_B)^2$	$\bar{A}(Y_B C_B)$
24.2	5	1 ms	9050 ± 70	970 ± 20	119 ± 8
24.2	10	1 ms	22600 ± 210	314 ± 25	236 ± 22
24.2	2	1 ms	-	130 ± 13	70 ± 10
Cosmics		1 ms	6500 ± 30	165 ± 0.1	13.1 ± 0.1

Table Va

Counting rates in Run 4 (per 1000 bursts). The target was Be. $\bar{A}$ stands for anticoincidence with F,T,L, and R. C_TY_T means total C and total Y, i.e., $C_B + C_L + C_R$ and $Y_B + Y_L + Y_R$.

PS energy (GeV)	Target	Gate	$(C_TY_T)^1$	$\bar{A}(C_TY_T)^1$	$(C_BY_B)^1$	$\bar{A}(C_BY_B)^1$	$(C_TY_T)^2$	$\bar{A}(C_TY_T)^2$	$(C_BY_B)^2$	$\bar{A}(C_BY_B)^2$	from traces $\bar{A}(C_TY_T)^2$	from traces $\bar{A}(C_BY_B)^2$
22.2	5	0.5 ms	10015 ± 70	8650 ± 66	3500 ± 30	2360 ± 24	390 ± 14	32.5 ± 4	381 ± 9	15.8 ± 2	15.5 ± 2	8 ± 1.4
20.0	5	0.5 ms	2470 ± 50	2010 ± 45	-	-	93 ± 10	20.4 ± 4.5	-	-	8.3 ± 3	-
20.0	5	1 ms	2360 ± 46	2120 ± 43	-	-	79 ± 8.5	17.2 ± 4.5	-	-	7.4 ± 3	-
Cosmics		1 ms	460 ± 9	330 ± 7	310 ± 2	245 ± 2	35 ± 2	19.6 ± 1.2	9.5 ± 0.3	2.1 ± 0.13	11.4 ± 1	1 ± 0.1

Table V b

Analysis of oscilloscope traces in Run 4.

PS energy (GeV)	Target	Trigger Signature	Anticounter percentage of total number of triggers				% of ν-like events	Counter combinations of ν-like events (%)		
			F	T	L	R		$(Y_BC_B)^2$	$(Y_LC_L)^2$	$(Y_RC_R)^2$
22.2	5	$\bar{A}(C_TY_T)^2$	17	1.5	2	-	57	70	9	14
22.2	5	$\bar{A}(C_BY_B)^2$	30	5	6	3	41	100	-	-
20.0	5	$\bar{A}(C_TY_T)^2$	3	3	3	5	57	82	-	14
Cosmics		$\bar{A}(C_TY_T)^2$	-	1	1	6	60	56	3	32
Cosmics		$\bar{A}(C_BY_B)^2$	2	4	3	18	49	100	-	-

FIGURE CAPTIONS

Fig. 1 : Shielding conditions in Run 1. The part hatched-inclined to the left was added during the run.

Fig. 2 : The shielding during Run 2.

Fig. 3 : Shielding during Runs 3 and 4. The parts added after Run 2 are drawn in black. Suspected weak points are indicated with the letters A, B, C and X.

Fig. 4 : The short sandwich as used in Run 1. The small phototubes on the front side of the Čerenkov counter C exclude particles entering the set-up from behind. (This signal is denoted by C_b in the tables.)

Fig. 5 : The short sandwich as used in Run 2.

Fig. 6 : The counter-controlled cloud chamber as used in Run 4. (In Run 3 the TOP-counter and the two side Čerenkov counters, C_L and C_R, were missing.)

Fig. 7 : Muon fluxes as a function of PS energy at a fixed shielding thickness corresponding to a momentum cut-off at 17.7 GeV/c. (1 burst = 2.1×10^{11} circulating protons in Figs. 7 - 9.)

Fig. 8 : Muon fluxes at 24.3 GeV PS energy as a function of shielding thickness.

Fig. 9 : "Neutrino-like" triggers $\bar{F}\bar{T}(Y_1\, Y_2\, C)^3$ as a function of shielding thickness. The curve labelled "expected muon flux" refers to the calculation of Ref. 4).

Fig. 10 : Background as function of PS energy.

1896/NP/kw

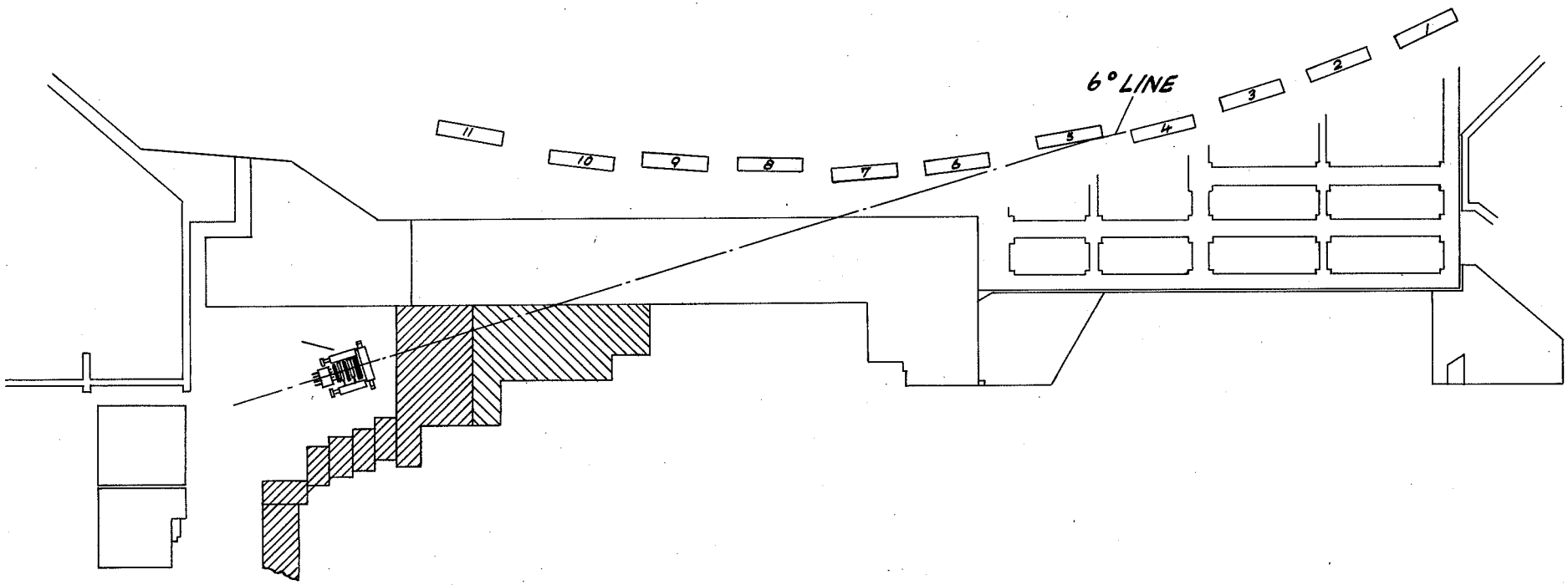

FIG. 1 LAYOUT OF 1st PRE-RUN

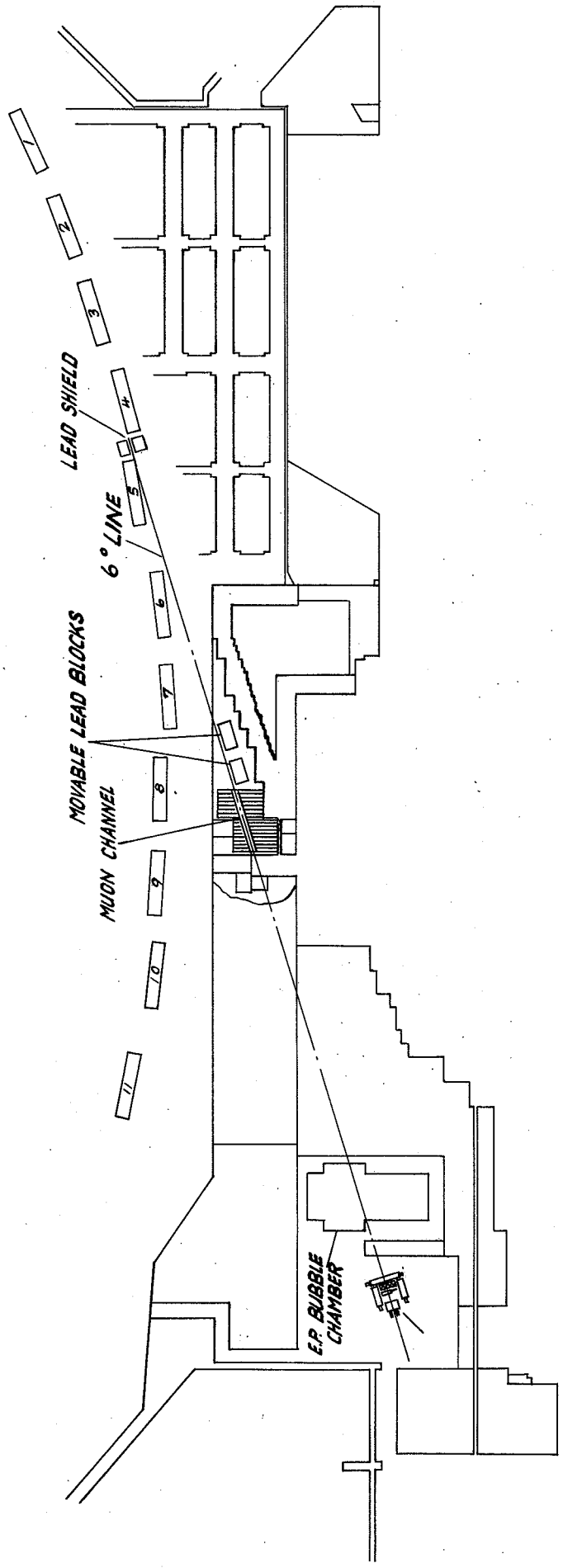

FIG. 2 LAYOUT OF 2nd PRE-RUN

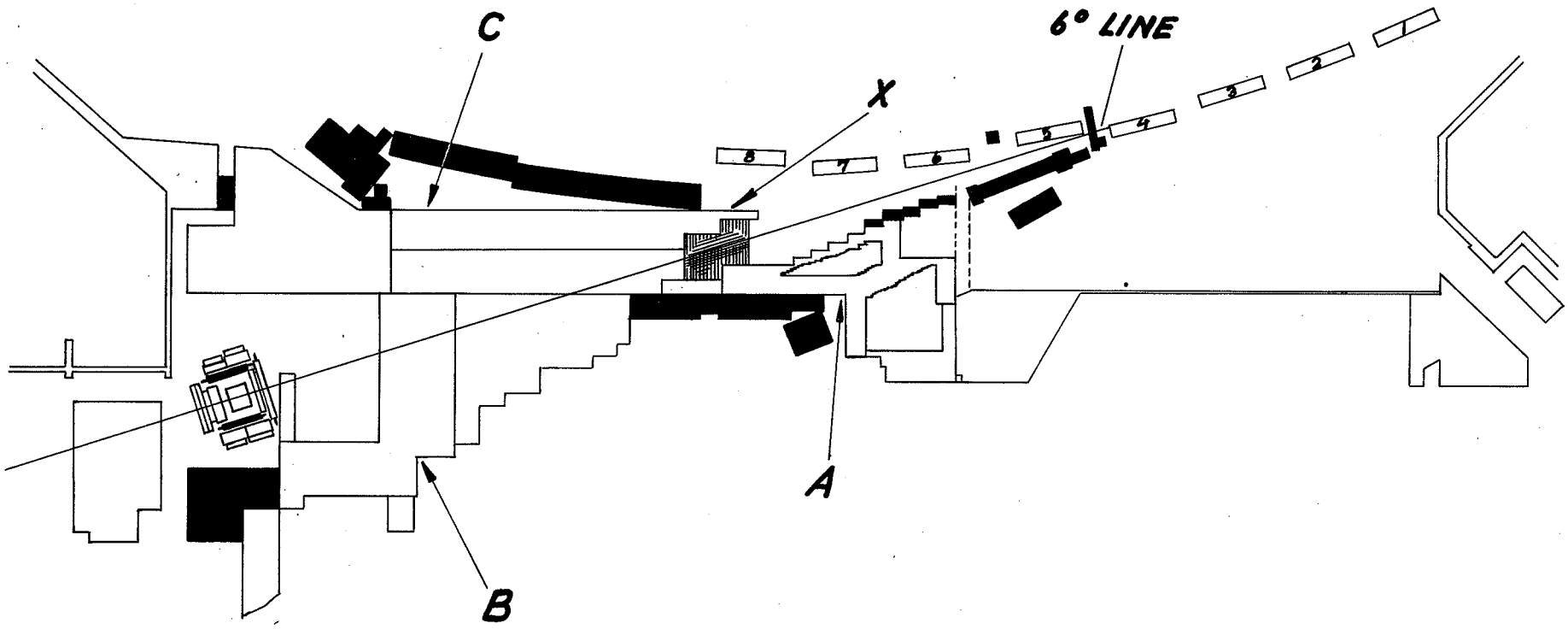

FIG. 3 SHIELDING ADDED BETWEEN 2nd AND 3rd PRE-RUN

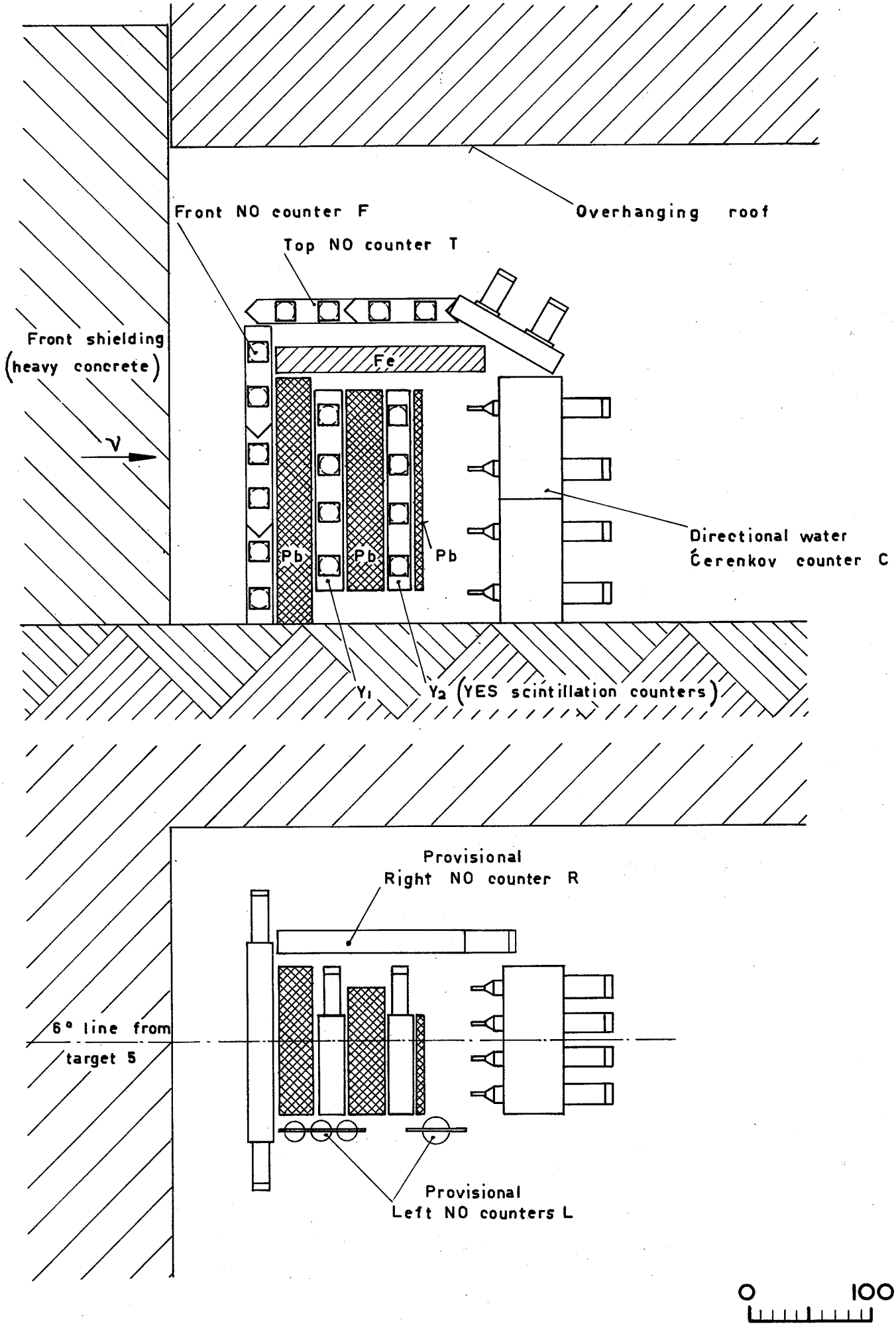

FIG. 4 THE SHORT SANDWICH
AS USED IN RUN I

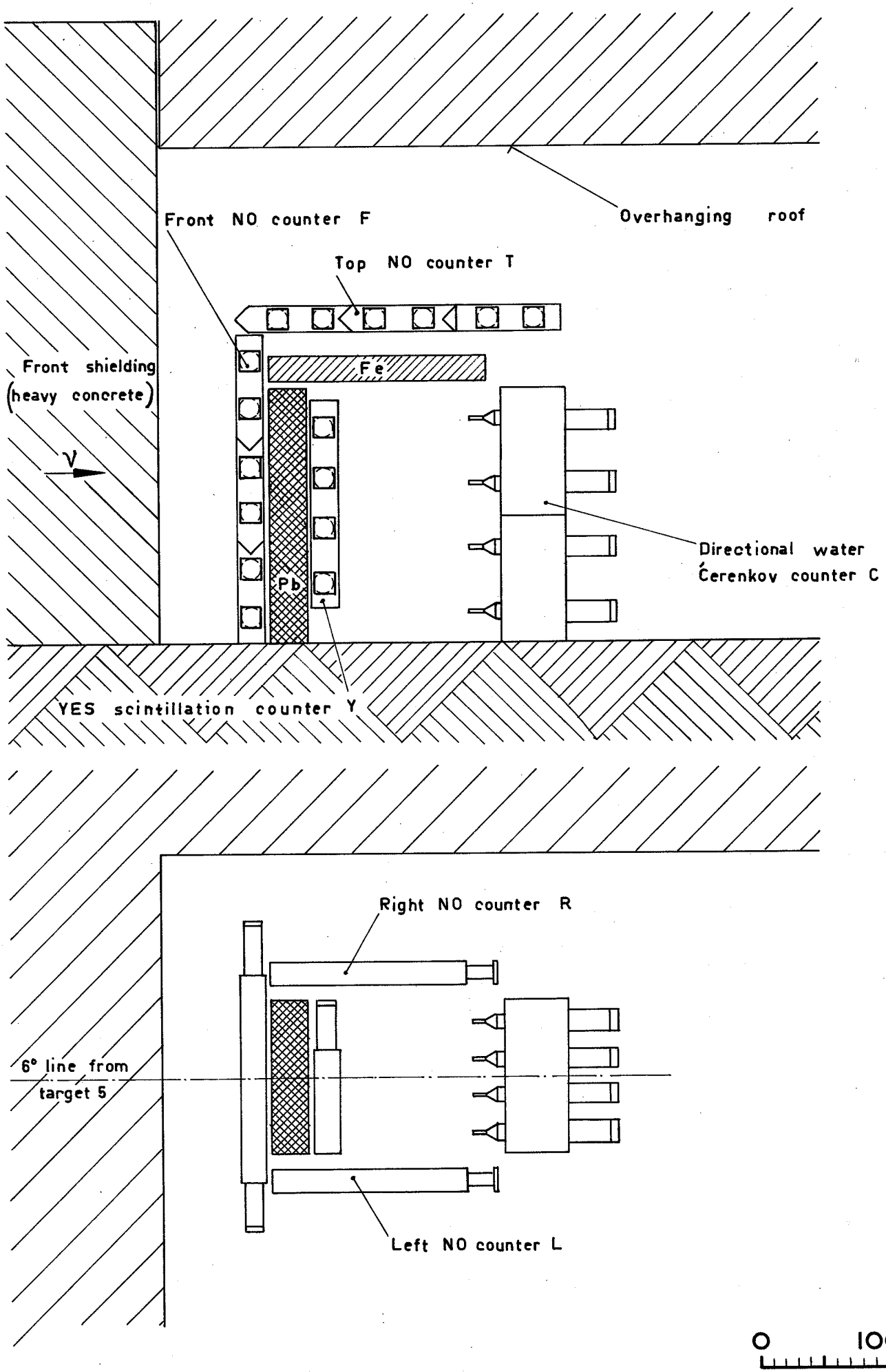

FIG. 5 THE SHORT SANDWICH
AS USED IN RUN 2

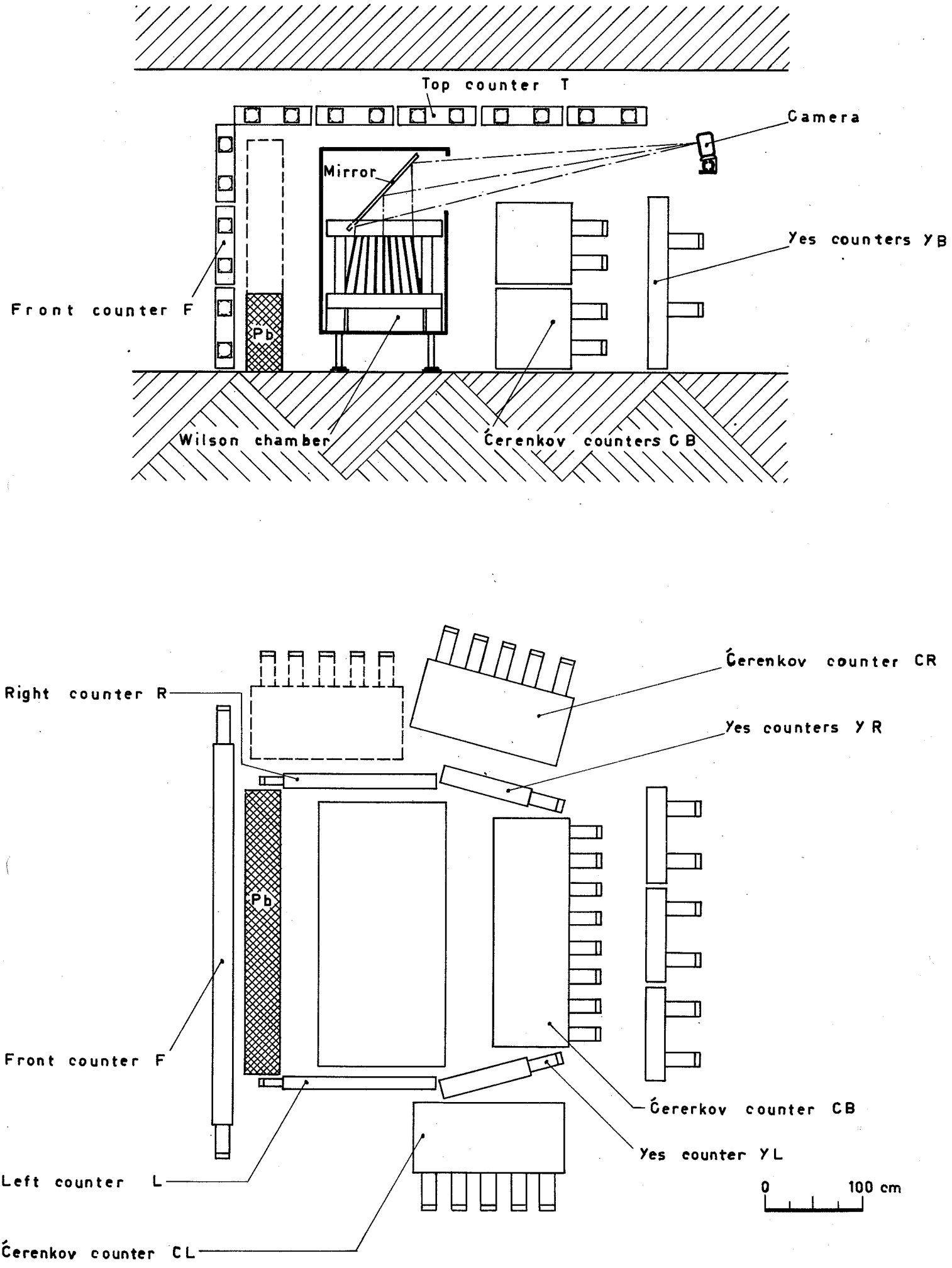

SIS/R/2984

FIG.6 THE COUNTER CONTROLLED WILSON CHAMBER

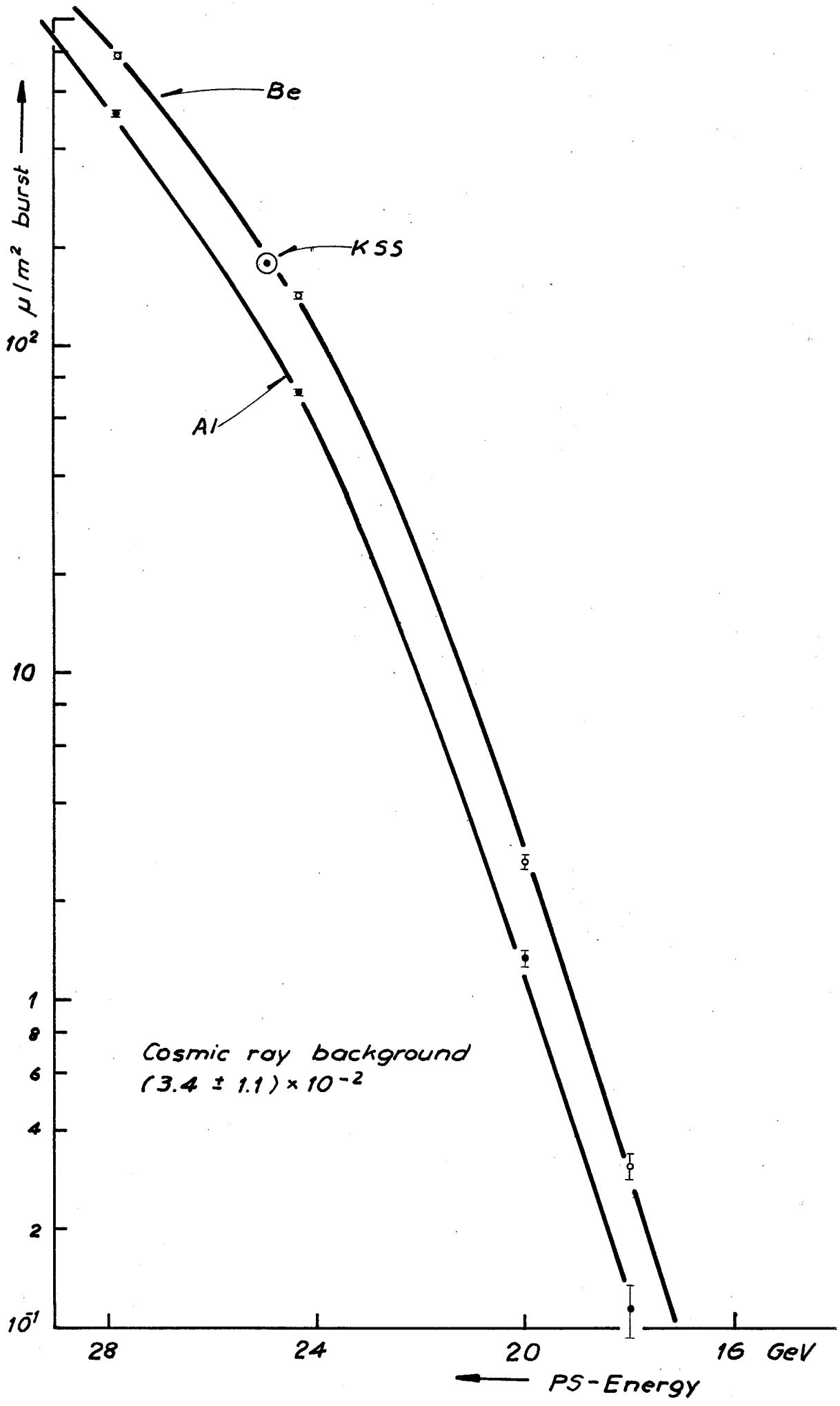

Fig. 7 Muon fluxes as a function of PS-Energy

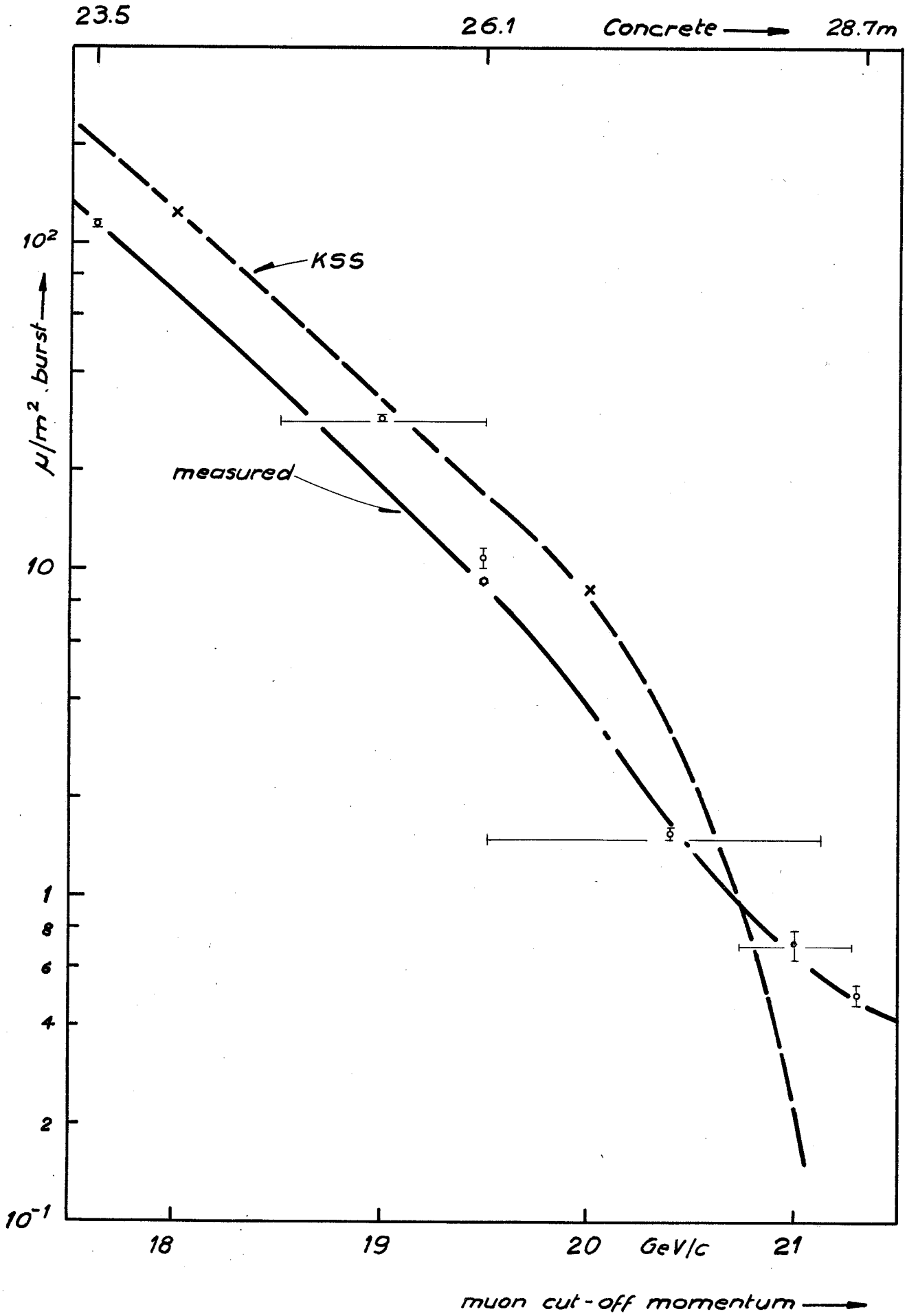

Fig. 8 Muon fluxes at 24.3 GeV PS-energy (Be) as a function of shielding

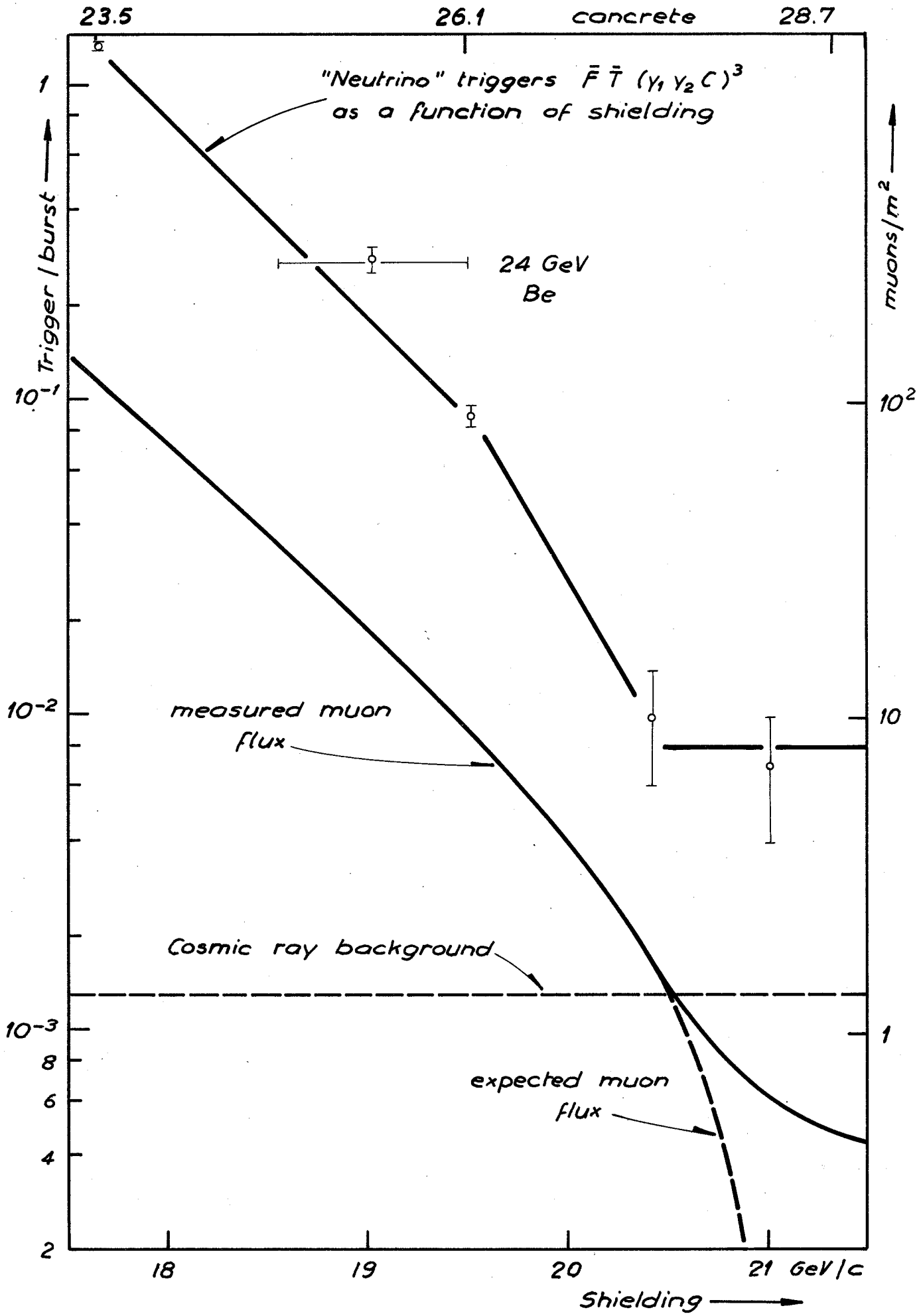
23.5
26.1
concrete
28.7
"Neutrino" triggers $\bar{F}\,\bar{T}\,(\gamma_1\,\gamma_2\,C)^3$
as a function of shielding
24 GeV
Be
Trigger / burst
muons/m²
1
10^{-1}
10^{-2}
10^{-3}
8
6
4
2
10^2
10
1
measured muon
flux
Cosmic ray background
expected muon
flux
18
19
20
21 GeV/c
Shielding

Fig. 9

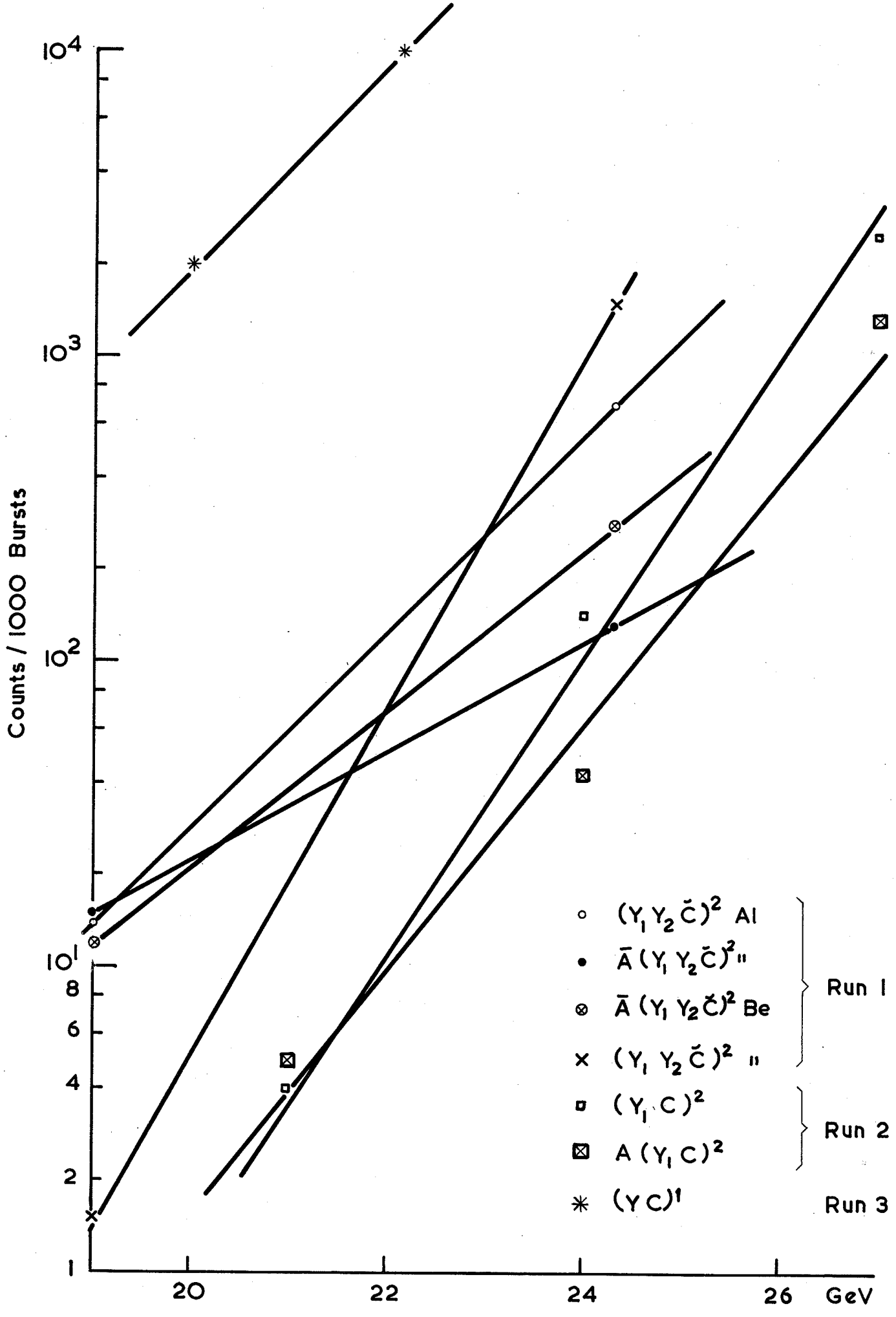

FIG. 10 Background as Function of PS-Energy

SIS/R/2987